

# Geotechnical properties of cement-stabilised fill material: Developing a linear regression model for predicting unconfined compression strength and undrained shear stress

Muntasir Ahmed, Mostakim Ahmed, Lubaba Afzal\*

Civil Engineering Department, Bangladesh University of Engineering and Technology, Dhaka-1000, Bangladesh

Received 7 November 2023; revised 18 December 2023; accepted 15 February 2024

## **Abstract:**

The use of cement stabilisation is considered a practical and cost-effective method in the construction sector for enhancing the geotechnical properties of fill materials. This research has the potential to introduce significant innovations in soil stability and strength, which are crucial for the design and construction of various geotechnical structures, such as foundations, embankments, and retaining walls. This study observed changes in unconfined compressive strength (UCS) and undrained shear stress (USS) by varying the percentage of cement content and curing period. Comprehensive geotechnical characterisation was conducted, including specific gravity determination, sieve analysis, maximum and minimum density tests, standard and modified Proctor compaction tests, and unconfined compression testing. Results were analysed and visualised through graphical representations. Cement content (2-7%) and curing time (7-28 days) led to substantial increases in soil UCS and USS, ranging from 18 to 43% for UCS and 13 to 39% for USS. This research employs a linear regression model for predicting these results, which outperforms existing models. This model contributes to the body of geotechnical engineering knowledge and provides direction for further study and real-world applications in soil stabilisation. The research culminates in a compelling demonstration of the transformative impact of controlled increases in cement content and curing time on the geotechnical properties of silty-sand.

**Keywords:** cement stabilisation for construction, compaction test, linear regression model, unconfined compressive strength, undrained shear stress.

**Classification numbers:** 4.2, 4.3

## **1. Introduction**

Unconfined compressive strength and undrained shear stress are two important properties for cement stabilisation that indicate the material's ability to resist deformation and failure under load. Cement-stabilised soil serves as a building material that possesses sufficient strength and durability while having low embodied energy [1]. The use of cement-stabilised soil in construction can address some of the challenges associated with earth construction, such as shrinkage cracking, low strength, and lack of durability [2]. Determining the engineering properties of soil for dynamic stability analysis remains a significant challenge [3]. The unconfined compressive strength test reveals that as the blending ratio increases, the axial strain reduces and brittle fracture becomes more evident. An empirical relationship accounting for the combined effects of cement mixing proportion and curing time is developed to determine UCS and USS. Several methods, including the addition of adhesive materials like cement and lime, are employed to strengthen loose soils for construction; each of these additives has its own economic, environmental, and practical considerations [4]. Saturated sands, often found in coastal areas, experience volumetric instability and significant deformation under seismic pressure, a phenomenon known as liquefaction [5]. For problematic sands, soil improvement is achieved using cement [6]. It is essential to determine the particle size distribution of sand for a

wide range of engineering applications. Significant properties such as setting time, hydration heat curves, water demand, adsorption properties, flowability performance, and compressive strength may vary among cement types with different particle size distributions, even if they have the same Blaine fineness [7-10]. Recent advancements have been made in understanding the influence of grain size on erosion potential. However, relatively few studies have quantified the effects of various geotechnical properties, despite their potential to significantly affect the mechanisms governing the erosion of coarse-grained soil particles. Silty sand has lower shear strength than pure sand because the fine silt particles reduce interparticle friction. Cementitious products are formed as a result of hydration interactions between cement and water during the curing process. These hydration by-products, such as calcium hydroxide (CH) and calcium silicate hydrates (C-S-H), help the cement-mixed sand build interparticle connections and gain strength [11].

The objective of this research is to elucidate the correlation between cement content and curing time on the geotechnical properties of stabilised soil, supported by results from various tests, including specific gravity, sieve analysis, maximum and minimum density, compaction, and unconfined compression strength tests. Existing research indicates that a large amount of test data is needed as predictor variables for a regression model to achieve desirable

\*Corresponding author: Email: lubaba.afzal@gmail.com

target variables. This article presents a prediction model that achieves high accuracy despite the limited availability of test data, providing more reliable predictions for undrained shear strength than unconfined compressive strength. This model could be useful for geotechnical engineers who need to estimate the strength and stability of sand-cement mixtures based on various inputs.

## 2. Materials and methods

### 2.1. Sample collection

Laboratory experiments were conducted to examine key stabilising elements. The water-cement ratio, mixing duration, and curing conditions were prioritised as they affect the performance of stabilised sand. Particle size distribution, specific gravity, maximum density, and minimum density were tested using standard procedures.

### 2.2. Physical properties tests

*Specific gravity test:* A representative sample was prepared, dried in an oven, submerged in water, and weighed. The specific gravity of the sample was determined according to ASTM D854.

*Sieve analysis:* The ASTM C136 test method encompasses sample preparation, sieve selection, sieving procedure, weighing, and particle size distribution analysis. The particle size distribution of aggregates was analysed to calculate the coefficient of uniformity ( $C_u$ ) and coefficient of curvature ( $C_c$ ).

*Maximum and minimum density test:* The accepted test procedure for measuring the maximum and minimum densities of soil samples is ASTM D4254. These densities are used to evaluate the stability and engineering behaviour of soils.

*Compaction test:* The soil sample was compacted in a cylindrical mould using a freely falling hammer from a specific height to determine the optimal moisture content and maximum dry density. Fifteen samples were prepared, comprising five separate 2.5 kg samples, each receiving five different additions of water, and were subjected to three distinct experiments or different compaction energies (Table 1).

**Table 1. Procedure of compaction tests.**

Test type	Mold size	Weight of Hammer (lb)	Number of layers	Height of Hammer drop (in)	Number of blows per layer	Compactive energy per layer (ft-lb/ft)
15 Blow proctor	4.6" height x 4.0" diameter	5.5	3	12	15	7400
Standard proctor	4.6" height x 4.0" diameter	5.5	3	12	25	12375
Modified proctor	4.6" height x 4.0" diameter	10	5	18	25	56300

*Specimen for unconfined compression test:* Air-dried silty sand with 2, 5, and 7% cement content was compacted at optimum moisture using the standard proctor method. The specimens were then extruded and trimmed to a diameter of 1.5" and a height of

3". A total of 12 different specimens were water-cured for 7, 14, and 28 days, and unconfined compression tests were performed to compare and observe variations in the results for each case (i.e., cement content and curing period).

*Procedure of unconfined compression test:* This test was conducted according to ASTM D2166. After being removed from the moist curing environment, stabilised samples were subjected to a uniform and shock-free force in a compression testing apparatus, deforming at a rate of approximately 0.05 inches (1 mm) per minute until failure. The entire load and associated deformation were recorded. Untreated samples were later evaluated in compression after the preparation phase (Fig. 1).



**Fig. 1. Unconfined compression test (UCS).**

### 2.3. Determining the undrained shear stress

If the unconfined compression test results are known, the undrained shear stress can be easily calculated using the formula:

$$S_u = Q_u/2$$

where  $S_u$  is the undrained strength;  $Q_u$  denotes unconfined compressive strength of soil. The angle of internal friction is obtained as  $\phi=0$  for the test. These specific conditions lead some engineers to refer to this test as an “unconsolidated undrained” test or UU for short [12].

### 2.4. Regression analysis

A multivariate regression model was developed to predict  $Q_u$  and  $S_u$  based on the percentage of cement content and curing period. Due to the limited dataset, synthetic data were generated to enhance model accuracy and minimise error. The model aligns with J.J. Binder’s (1985) [13] multivariate regression approach and exhibits characteristics of a first-order unbiased mean squared error estimator [14]. To evaluate model performance, the mean actual error and coefficient of determination were calculated.

### 3. Results and discussion

#### 3.1. Grain size distribution

The  $D_{60}$ ,  $D_{30}$ , and  $D_{10}$  values, derived from the soil gradation curve, correspond to the particle diameters at which 60, 30, and 10% of the soil's total mass, respectively, is composed of finer particles. The results obtained from sieve analysis are displayed in Table 2.

Table 2. Values from sieve analysis.

Parameter	Value
$D_{60}$ (mm)	0.28
$D_{30}$ (mm)	0.15
$D_{10}$ (mm)	0.09
Coefficient of uniformity, $C_u$	3.11
Coefficient of curvature, $C_c$	0.89

As the coefficient of uniformity  $C_u=3.11 < 6$  and  $C_c=0.89 < 1$ , along with a silt content of 7% (which is between 5 and 12%), the soil is classified as SP-SM, meaning poorly graded sand with silt. According to the correlations found, the gradation of the silty sand impacts the strength outcomes of cement-stabilised sand.

#### 3.2. Compaction test

Both the standard proctor test and modified proctor tests were performed on the soil sample. The results from each test and a comparison between the values are discussed in the following subsections.

#### 3.3 Standard proctor test

The standard proctor test produced a value for the optimal moisture content (OMC), which is the moisture content at which the material reaches its maximum dry density under the given compaction effort. The results of the standard proctor test are displayed in Table 3.

Table 3. Results from both compaction methods.

Parameters	Standard proctor test	Modified proctor test
Optimum moisture content, OMC (%)	14.3	13.7
Maximum dry density ( $\text{kN/m}^3$ )	15.9	16.7

#### 3.4. Modified proctor test

In the modified proctor test, the optimal moisture content (OMC) denotes the moisture content at which the soil sample achieves maximum compaction due to the greater compaction energy applied. At this moisture level, soil particles are properly lubricated, enabling effective compaction and maximum density. The OMC for the modified proctor test is typically lower than that for the standard proctor test because the greater compaction energy in the modified proctor test breaks down more soil particles, creating additional water voids that need to be filled to achieve maximum compaction (Fig. 2). The

modified proctor method uses a heavier hammer and a greater drop distance compared to the standard proctor method. This increased compaction energy results in a denser soil structure with a higher unit weight [15]. The optimum moisture content and maximum dry density resulting from the modified proctor test is shown in Table 3.

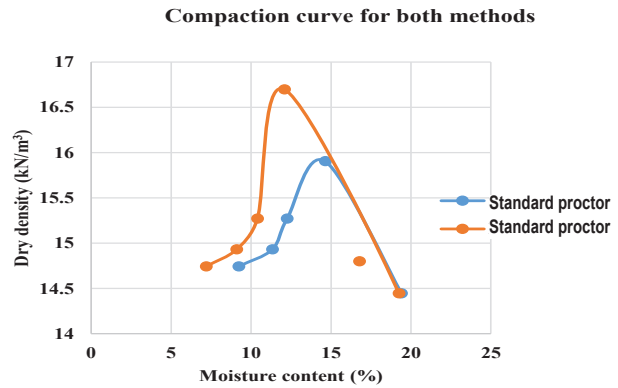


Fig. 2. Dry density in both standard and modified proctor tests.

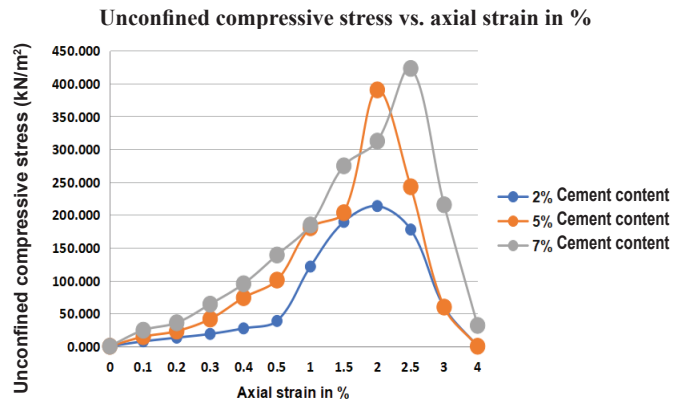


Fig. 3. Unconfined compressive stress ( $\text{kN/m}^2$ ) vs. axial strain (%) for 7 curing days with different cement contents.

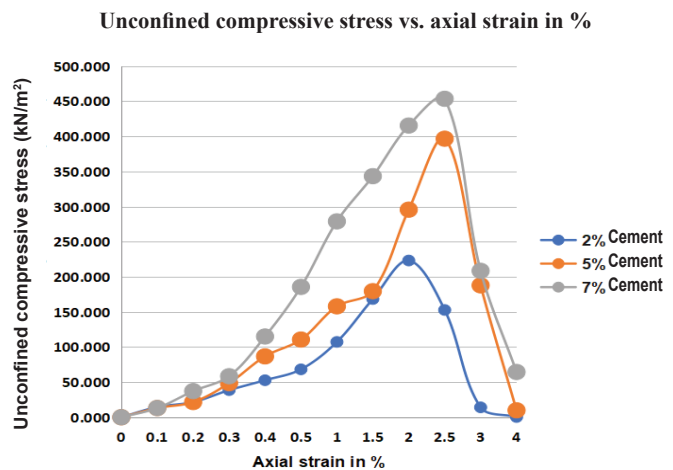


Fig. 4. Unconfined compressive stress ( $\text{kN/m}^2$ ) vs. axial strain in % for 14 curing days with different cement contents.

Unconfined compressive stress vs. axial strain in %

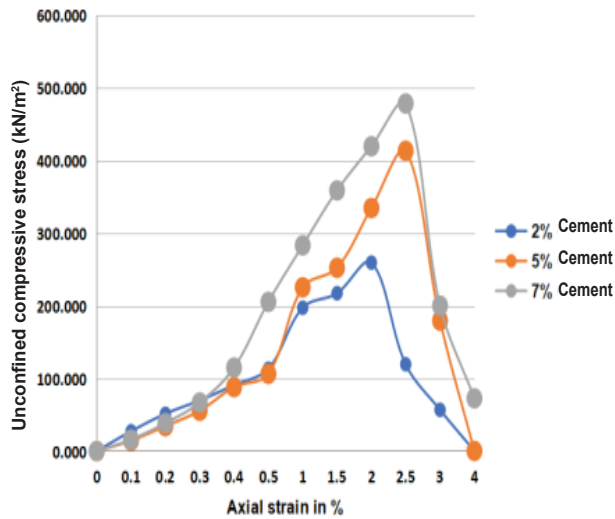


Fig. 5. Unconfined compressive stress (kN/m<sup>2</sup>) vs. axial strain in % for 28 curing days with different cement contents.

The three graphs (Figs. 3-5) presented depict the relationship between unconfined compressive strength and axial strain (%) for different curing days and cement contents. The graphs indicate that as the cement content increases, the peak unconfined compressive strength also rises, resulting in enhanced load-bearing capacity. This trend is consistent across curing periods of 7, 14, and 28 days [16].

The unconfined compressive strength test shows that as the cement blending ratio increases, the axial strain decreases and brittle fracture becomes more pronounced. An empirical relationship accounting for the combined effects of cement mixing proportion and curing time has been developed to determine  $Q_u$  and  $S_u$ .

Figures 6 and 7 show that both  $Q_u$  and  $S_u$  increase with the curing period, indicating that the material becomes stronger and more resistant to deformation over time. This is due to the ongoing cement hydration reaction, which produces more gels that fill the pores and bond the soil particles.

Figures 8 and 9 show that both  $Q_u$  and  $S_u$  increase with cement content, suggesting that the material becomes stronger

$Q_u$  (kN/m<sup>2</sup>) vs. curing period (in days)

with 2%,5%,7% cement

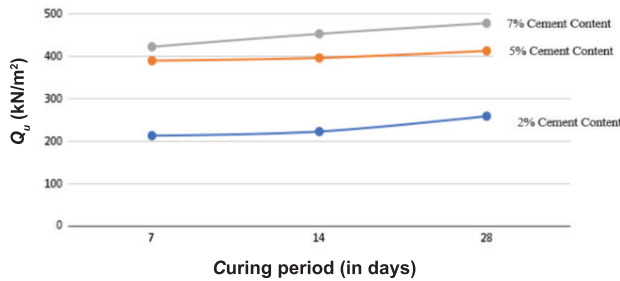


Fig. 6. Unconfined compressive stress  $Q_u$  (kN/m<sup>2</sup>) vs. curing period.

$S_u$  (kN/m<sup>2</sup>) vs. curing period (in days)

with 2%,5%,7% cement

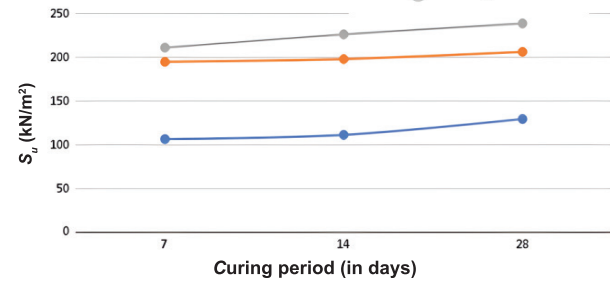


Fig. 7. Undrained shear strength  $S_u$  (kN/m<sup>2</sup>) vs. curing period (days).

$S_u$  (kN/m<sup>2</sup>) vs. cement (%)

Line for 7days,14 days & 28 days

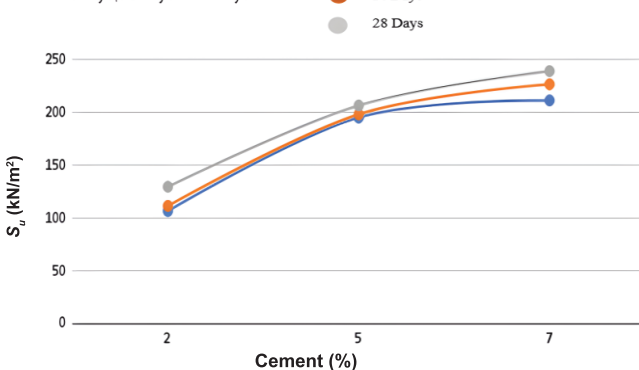


Fig. 8. Undrained shear strength  $S_u$  (kN/m<sup>2</sup>) vs. cement content (%).

$Q_u$  (kN/m<sup>2</sup>) vs. cement (%)

Line for 7days,14 days & 28 days

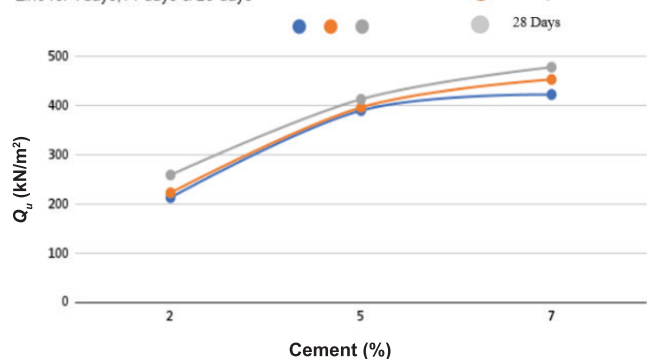


Fig. 9. Unconfined compressive stress  $Q_u$  (kN/m<sup>2</sup>) vs. cement content (%).

and more resistant to failure with higher cement content. This improvement is attributed to the additional cementitious material, which enhances the cohesion and friction within the soil matrix.

3.5. Tabular summary of values from unconfined compression test

Table 4 illustrates a noteworthy trend: for a consistent curing period, an increase in cement content from 2 to 5% results in a substantial rise in unconfined compressive strength. Interestingly, the increase in undrained shear stress due to a higher cement percentage is less pronounced compared to the rise in unconfined compressive strength. Moreover, transitioning from 5 to 7% cement content results in a slower rate of increase in both  $Q_u$  and  $S_u$  compared to the previous change from 2 to 5%. This suggests a nuanced relationship between cement content and curing period, reflecting complex changes in these mechanical properties.

Table 4. Results from unconfined compression test.

Cement content	2%			5%			7%		
	7	14	28	7	14	28	7	14	28
$Q_u$ (kN/m <sup>2</sup> )	213.42	223.17	259.38	390.30	396.62	413.25	422.95	453.43	478.48
$S_u$ (kN/m <sup>2</sup> )	106.71	111.58	129.69	195.15	198.31	206.62	211.47	226.71	239.24

3.6. Result of regression analysis

The regression analysis conducted in this research was evaluated using statistical metrics for the correlation coefficient ( $R$ ) (Figs. 10, 11). Table 5 contains the mean absolute error (MAE), mean squared error (MSE), and  $R^2$  value of  $Q_u$  and  $S_u$ , respectively.

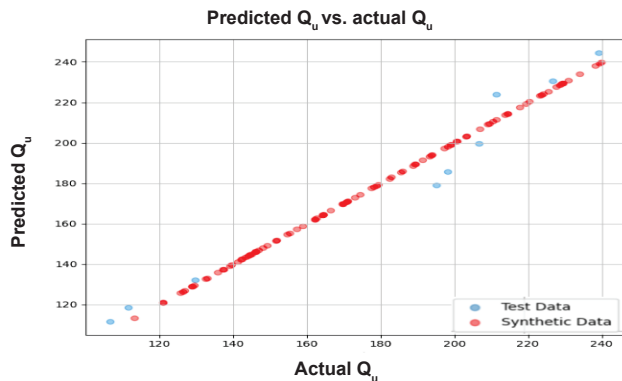


Fig. 10. Prediction analysis of unconfined compression test.

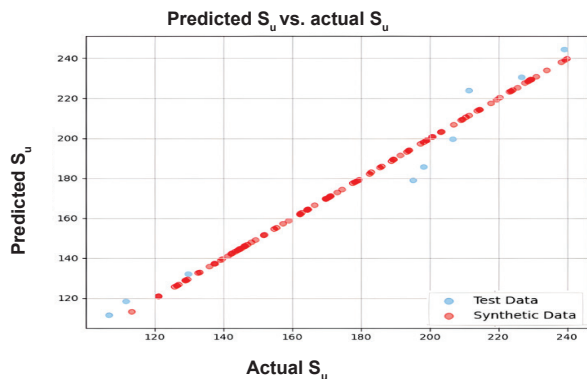


Fig. 11. Prediction analysis of undrained shear stress.

Table 5. Result of regression analysis.

	Mean absolute error	Mean squared error	$R^2$
$Q_u$	15.91	329.97	0.96
$S_u$	7.95	82.51	0.96

*Mean absolute error:* The MAE provides a quantitative measure of the average difference between the model’s predictions and the actual values. An MAE of 15.91 kN/m<sup>2</sup> for  $Q_u$  indicates that, on average, the model’s predictions for  $Q_u$  deviate from the actual values by approximately 15.91 kN/m<sup>2</sup>. Similarly, an MAE of 7.95 kN/m<sup>2</sup> for  $S_u$  suggests that the average prediction error for  $S_u$  is around 7.95 kN/m<sup>2</sup>. The lower value of MAE for  $S_u$  implies that the model’s predictions for  $S_u$  are closer to the actual values compared to that of  $Q_u$ .

*Mean squared error:* The MSE measures the average squared difference between the model’s predicted values and the actual values. A significantly higher MSE for  $Q_u$  (329.97) compared to that of  $S_u$  (82.51) suggests greater variability in the predictions or potential outliers affecting the model’s performance for  $Q_u$ . This is because MSE is sensitive to outliers and large errors, magnifying their impact on the overall error measure. Conversely, the lower MSE for  $S_u$  implies that the model’s predictions for  $S_u$  are more consistent and less prone to outliers.

*Coefficient of determination:* The  $R^2$  statistic quantifies the proportion of the variance in the dependent variable that is explained by the independent variables in a regression model. An  $R^2$  value close to 1 indicates a perfect fit, meaning that the regression predictions perfectly align with the observed data.

The high  $R^2$  values of 0.96 for both  $Q_u$  and  $S_u$  indicate that the model explains approximately 96% of the variability in the respective target variables. This suggests a strong correlation between the selected features (cement content and curing days) and the target variables ( $Q_u$  and  $S_u$ ).

4. Conclusions

A synergistic effect was observed with increases in cement content typically resulting in a 30-40% enhancement in strength and load-bearing capacity. This suggests that the addition of cement improves the strength and load-bearing capacity of the stabilised sand. As a binding agent, cement particles create a matrix that is more cohesive and improves particle interlocking, leading to increased compressive stress. The sand-cement mixture exhibited a significantly higher undrained shear strength with both longer curing times and higher cement content. On average, increasing the curing period led to a 20-30% increase in undrained shear strength. This enhancement is attributed to the cement’s adhesive properties, which improve frictional resistance and inter-particle bonding. These findings indicate that stabilised sand is better able to withstand shear stresses, making it more suitable for engineering applications where stability and resistance to deformation are critical.

The results of the compaction tests showed that the modified proctor test yielded a higher maximum dry density and a lower optimum moisture content compared to the standard proctor test for the same soil sample. This indicates that the modified proctor test is a more effective method for compacting soil and improving its strength and stability. Increasing cement content improves the engineering properties of high-plasticity soils, such as reducing their plasticity and shrink/swell potential, and increasing their bearing capacity. Cement stabilisation also enhances soil strength and durability by forming hydration products that bind the soil particles together.

Through controlled increases in both cement content and curing time, silty-sand exhibited significantly enhanced geotechnical properties, including dry density, undrained shear strength, and unconfined compressive strength. These findings have significant implications for geotechnical engineers and professionals involved in construction and soil stabilisation projects.

The prediction model developed in this research demonstrates superior performance compared to existing models. The model exhibits strong predictive capabilities, as evidenced by high  $R^2$  values for both output parameters, indicating a good fit between the model and the observed data. The prediction error for  $S_u$  is consistently lower than that for  $Q_u$  as measured by both MAE and MSE. This suggests that the model's predictive accuracy is higher for  $S_u$  compared to  $Q_u$ . Despite the relatively low prediction errors, it is important to consider the absolute magnitude of these errors in the context of the intended application. If precision is critical and the acceptable error threshold is very low, even these small errors may have significant consequences. This research underscores the pivotal role of optimised cement content and curing time in enhancing the geotechnical properties of silty-sand, paving the way for more resilient and sustainable construction and soil stabilisation projects.

## 5. Future works

If the higher MSE for  $Q_u$  is attributed to outliers or specific segments of the data where the model's performance is suboptimal, further investigation and potential refinement of the model may be necessary to address these areas of deficiency. Overall, the model demonstrates notable robustness and can be considered reliable for predicting  $Q_u$  and  $S_u$  based on the provided inputs. However, it is noteworthy that the model's predictions for  $S_u$  are slightly more reliable compared to those for  $Q_u$ .

## CRedit author statement

Muntasir Ahmed: Conceptualisation, Methodology, Laboratory testing, Data collection, Data analysis, Visualisation, Revision, Original draft preparation, Reviewing and Editing; Mostakim Ahmed: Conceptualisation, Methodology, Laboratory testing, Data collection, Data analysis, Visualisation, Revision, Original draft preparation, Reviewing and Editing; Lubaba Afzal: Conceptualisation, Methodology, Laboratory testing, Data collection, Data analysis, Visualisation, Revision, Original draft preparation, Reviewing and Editing.

## ACKNOWLEDGEMENTS

The authors would like to express their gratitude to Dr. Abu Siddique and the Geotechnical Engineering Laboratory of Bangladesh University of Engineering and Technology.

## COMPETING INTERESTS

The authors declare that there is no conflict of interest regarding the publication of this article.

## REFERENCES

- [1] K.K.G.K.D. Kariyawasam, C. Jayasinghe (2016), "Cement stabilized rammed earth as a sustainable construction material", *Construction and Building Materials*, **105**, pp.519-527, DOI: 10.1016/j.conbuildmat.2015.12.189.
- [2] R. Bahar, M. Benazzoug, S. Kenai, (2004), "Performance of compacted cement-stabilised soil", *Cement and Concrete Composites*, **26(7)**, pp.811-820, DOI: 10.1016/j.cemconcomp.2004.01.003.
- [3] W.F. Marcuson, P.F. Hadala, R.H. Ledbetter (1996), "Seismic rehabilitation of earth dams", *Journal of Geotechnical Engineering*, **122(1)**, DOI: 10.1061/(ASCE)0733-9410(1996)122:1(7).
- [4] S. Talamkhani (2023), "Machine learning-based prediction of unconfined compressive strength of sands treated by microbially-induced calcite precipitation (MICP): A gradient boosting approach and correlation analysis", *Advances in Civil Engineering*, DOI: 10.1155/2023/3692090.
- [5] H.M. Abasi, B. Kordtabar, A. Kordnaei (2018), "Liquefaction prediction using CPT data by triangular chart identification", *International Journal of Geotechnical Engineering*, **12(4)**, pp.377-382, DOI: 10.1080/19386362.2017.1282399.
- [6] H. MolaAbasi (2023), "Novel estimation of time-dependent unconfined compressive strength of sand treated with cement and zeolite", *Geotechnical and Geological Engineering*, **41(5)**, pp.3217-3224, DOI: 10.1007/s10706-023-02428-2.
- [7] J. Assaad, S. Asseily, J. Harb (2010), "Effect of grinding aids on the clinker factor and energy consumption of Portland cement", *ACI Mater. J.*, 30pp.
- [8] M. Katsioti, P.E. Tsakiridis, P. Giannatos, et al. (2009), "Characterization of various cement grinding aids and their impact on grindability and cement performance", *Construction and Building Materials*, **23(5)**, pp.1954-1959, DOI: 10.1016/j.conbuildmat.2008.09.003.
- [9] Y.M. Zhang, T.J.N. Munn (1995), "Effects of particle size distribution, surface area and chemical composition on Portland cement strength", *Powder Technology*, **83(3)**, pp.245-252, DOI: 10.1016/0032-5910(94)02964-P.
- [10] D.P. Bentz, E.J. Garboczi, C.J. Haecker, et al. (1999), "Effects of cement particle size distribution on performance properties of Portland cement-based materials", *Cement and Concrete Research*, **29(10)**, pp.1663-1671, DOI: 10.1016/S0008-8846(99)00163-5.
- [11] M. Ghanbari, M. Bayat (2022), "Effectiveness of reusing steel slag powder and polypropylene fiber on the enhanced mechanical characteristics of cement-stabilized sand", *Civil Engineering Infrastructures Journal*, **55(2)**, pp.241-257, DOI: 10.22059/CEIJ.2021.319310.1742.
- [12] O. Gunaydin, A. Gokoglu, M. Fener (2010), "Prediction of artificial soil's unconfined compression strength test using statistical analyses and artificial neural networks", *Advances in Engineering Software*, **41(9)**, pp.1115-1123, DOI: 10.1016/j.advengsoft.2010.06.008.
- [13] J.J. Binder (1985), "On the use of the multivariate regression model in event studies", *Journal of Accounting Research*, **23(1)**, pp.370-383, DOI: 10.2307/2490925.
- [14] S. Chen, P. Lahiri (2008), "On mean squared prediction error estimation in small area estimation problems", *Proceedings of The Survey Research Methods Section*, **37(11)**, pp.1792-1798.
- [15] J. Connelly, W. Jensen, P. Harmon (2008), *Proctor Compaction Testing*, <https://core.ac.uk/download/pdf/77939216.pdf>, accessed 10 October 2023.
- [16] W.A. Jabban, J. Laue, S. Knutsson, et al. (2019), "A comparative evaluation of cement and by-product petrit T in soil stabilization", *Applied Sciences*, **9(23)**, DOI: 10.3390/app9235238.